

DERMAE: IMPROVING SKIN LESION CLASSIFICATION THROUGH CONDITIONED LATENT DIFFUSION AND MAE DISTILLATION

Francisco Filho Kelvin Cunha Fábio Papais Emanuel dos Santos Rodrigo Mota
Thales Bezerra Erico Medeiros Paulo Borba Tsang Ing Ren

Centro de Informática, Universidade Federal de Pernambuco, Brazil

ABSTRACT

Skin lesion classification datasets often suffer from severe class imbalance, with malignant cases significantly under-represented, leading to biased decision boundaries during deep learning training. We address this challenge using class-conditioned diffusion models to generate synthetic dermatological images, followed by self-supervised MAE pretraining to enable huge ViT models to learn robust, domain-relevant features. To support deployment in practical clinical settings, where lightweight models are required, we apply knowledge distillation to transfer these representations to a smaller ViT student suitable for mobile devices. Our results show that MAE pretraining on synthetic data, combined with distillation, improves classification performance while enabling efficient on-device inference for practical clinical use.

Index Terms— Skin lesion classification, Synthetic Generation, Latent diffusion

1. INTRODUCTION

Skin cancer is among the most prevalent neoplasias worldwide, yet few patients actively seek or have access to specialized medical attention [1]. Initial assessments are often performed by general practitioners, who may struggle to reach accurate diagnoses without specialist support, while biopsies are invasive and typically avoided for suspected benign lesions. Moreover, the lack of centralized and standardized patient data, together with variability related to physical traits, geography, or ethnicity, contributes to biased dermatology datasets. As a result, most medical imaging datasets are small and highly imbalanced, leading deep learning models to favor majority classes and systematically misclassify underrepresented lesions [2]. This issue is particularly pronounced in dermatology, where benign lesions dominate. To alleviate this limitation, data augmentation techniques have been widely adopted [3]. Conventional methods rely on geometric and color transformations [4], but they are restricted to modifying existing samples and cannot introduce novel lesion patterns. Synthetic image generation has therefore emerged as a promising alternative [5, 3], with recent diffusion models [6] showing potential to mitigate class imbalance

through data synthesis [2]. Meanwhile, in classification, architectures such as the Vision Transformer (ViT) [7] have demonstrated powerful representation learning capabilities via self-attention; however, their strong dependence on large-scale data significantly limits their effectiveness on current dermatology datasets.

In this work, we address class imbalance in skin lesion classification using synthetic images generated by class-conditioned diffusion models. We introduce a pre-training strategy based on Masked Autoencoders (MAE), where the model is first trained on large-scale synthetic data to learn generalizable representations and supplement underrepresented malignant classes. To support deployment in resource-constrained clinical settings, we further apply knowledge distillation, using the MAE as a teacher to train smaller classifiers suitable for mobile devices. Experimental results demonstrate that synthetic pre-training combined with distillation improves classification performance while enabling compact, point-of-care dermatology models.

2. METHODOLOGY

2.1. Synthetic Data Generation

We evaluate our approach on the HAM10000 dermoscopic dataset [8], which contains 10,000 images from eight lesion categories, including three malignant classes. The dataset is highly imbalanced, with approximately 90% benign samples. To mitigate this imbalance, we augment the training data with synthetic images generated using a Denoising Diffusion Probabilistic Model (DDPM) [6]. Two generation strategies are considered: (i) **unconditional generation**, in which 600,000 samples are generated without class conditioning to model the overall lesion distribution; and (ii) **conditional generation**, where class embeddings are introduced during inference to explicitly balance malignant and benign classes.

The model employs a U-Net backbone [6] to parameterize the denoising function $\epsilon_\theta(\mathbf{x}_t, t)$, following the standard DDPM formulation [6]. The forward pass progressively corrupts a clean image \mathbf{x}_0 into a noisy latent variable \mathbf{x}_t through the addition of Gaussian noise (Equation 1). Where $\{\alpha_t\}_{t=1}^T$ follows a linear noise schedule with $T = 1000$ timesteps. Ini-

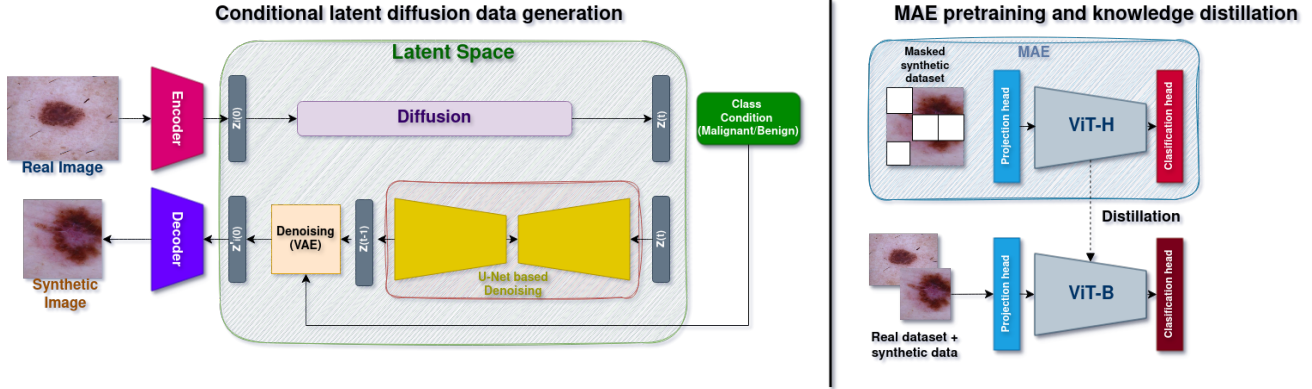


Fig. 1. Overview of the proposed framework. First, class-conditioned latent diffusion generates synthetic skin image. Next, the synthetic data is used to pretrain a ViT-H model using an MAE objective. Finally, knowledge distillation tunes a smaller student model from the pretrained ViT, which is fine-tuned using a combination of real and synthetic data.

tially, the model was trained to predict the noise component via the mean squared error objective, as in Equation 2.

$$q(\mathbf{x}_t | \mathbf{x}_0) = \mathcal{N}(\mathbf{x}_t; \sqrt{\alpha_t} \mathbf{x}_0, (1 - \alpha_t)\mathbf{I}) \quad (1)$$

$$\mathcal{L}_{MSE}(\theta) = \mathbf{E}_{\mathbf{x}_0, t, \epsilon \sim \mathcal{N}(0, \mathbf{I})} \left[\|\epsilon - \epsilon_\theta(\mathbf{x}_t, t)\|_2^2 \right] \quad (2)$$

To improve perceptual fidelity and reduce low-frequency artifacts commonly introduced by the MSE objective, we incorporated a perceptual loss term [9]. The final training objective is illustrated in Equation 3.

$$\mathcal{L}(\theta) = \mathcal{L}_{MSE}(\theta) + \lambda \mathcal{L}_{perc}(\theta) \quad (3)$$

Training was performed using the Adam optimizer (learning rate 1×10^{-4}), and resolution of 256×256 pixels. Sampling followed the standard stochastic DDPM denoising to retrieve synthetic samples from the learned distribution.

2.2. Self-supervised pre-training

To leverage both the original and synthetically generated data in a self-supervised manner, we employ a Masked Auto-encoder (MAE) [10] with a ViT-Huge backbone (ViT-H/16). The model employs a patch size of 16×16 , an embedding dimension of 1024, 24 transformer encoder layers, and 16 self-attention heads. During training, a random masking ratio of 75% is applied to the input patches, such that only a subset of visible tokens is processed by the encoder, while the decoder is tasked with reconstructing the missing patches. This reconstruction objective encourages the model to learn semantically meaningful latent representations that capture global lesion structures rather than low-level correlations. Formally, let $\mathbf{x} \in \mathbf{R}^{H \times W \times 3}$ denote an input image divided into N patches. A binary mask $M \in \{0, 1\}^N$ selects the subset

of visible patches for the encoder, yielding encoded tokens $z = f_\theta(\mathbf{x} \odot M)$, where f_θ is the ViT encoder. The decoder g_ϕ then reconstructs the original image patches $\hat{\mathbf{x}}$ from z and mask tokens. The training objective is a pixel-wise reconstruction loss over the masked regions, as shown in Equation 4.

$$\mathcal{L}_{MAE}(\theta, \phi) = \|\mathbf{x} - g_\phi(f_\theta(\mathbf{x} \odot M))\|_2^2 \odot (1 - M) \quad (4)$$

Training is performed for 100 epochs using the AdamW optimizer with cosine learning rate decay, using an initial learning rate of 1×10^{-4} , batch size of 256, and weight decay of 0.05. The MAE pretraining stage enables the learning of generalized visual features from the large synthetic data, alleviating the limitations imposed by imbalance. These learned representations are subsequently transferred to smaller downstream classification models through knowledge distillation, allowing compact models to benefit from the richer feature space acquired during MAE pretraining.

2.3. Knowledge distillation

To take advantage of the representational capabilities acquired during MAE pretraining, we combine self-supervised learning with knowledge distillation to transfer knowledge from the ViT-H model to a smaller student network. Specifically, the encoder of the pretrained MAE (ViT-H) is adopted, and its output representations are used to guide a ViT-Base (ViT-B/16) student model. The student architecture consists of 12 transformer layers, an embedding dimension of 768, and 12 self-attention heads. Knowledge transfer is performed using a soft-target distillation strategy, wherein the student is encouraged to match both the teacher’s output distribution and the ground-truth class labels. Let p_t denote the teacher’s predicted probability distribution and p_s the student’s output,

the distillation loss (\mathcal{L}_{KD}) is defined as in equation 5. \mathcal{L}_{CE} is the cross-entropy loss with ground-truth labels y , \mathcal{L}_{KL} is the Kullback–Leibler divergence between softened probability distributions, and α balances the contribution of soft and hard supervision. This distillation procedure enables the student network to inherit the high-level semantic structure and feature representations learned during MAE self-supervised pretraining. Our architecture is illustrated in Figure 1.

$$\mathcal{L}_{KD} = (1 - \alpha) \mathcal{L}_{CE}(p_s, y) + \alpha \mathcal{L}_{KL}(p_s, p_t) \quad (5)$$

2.4. Experiments details

Experiments were performed under three configurations to evaluate the effect of synthetic augmentation: (i) a **baseline** trained solely on HAM10000; (ii) **MAE + synthetic**, using MAE pre-training followed by training with synthetic samples to balance benign and malignant classes; and (iii) **distillation + augmentation (distill)**, combining real data with synthetic samples distilled from MAE pre-training.

The ViT-B/16 baseline was trained for 1000 epochs using AdamW (learning rate 3×10^{-5} , batch size 64, and weight decay 0.01) with a cosine scheduler. Results were evaluated using accuracy and F1-score [8, 5] and compared against EfficientNet variants [11] and Derm-t2im [5], which employs a Stable Diffusion-based framework for synthetic generation and subsequent binary classification.

3. EXPERIMENTS AND DISCUSSIONS

We trained EfficientNet and ViT baseline models using the original HAM10000 training split. From the 10,015 available samples, we allocate 80% for training (8,012) and 20% for validation (2,003), retaining the original test set (1,512 images) for evaluation. It is important to note that the same training set is used for optimizing synthetic image generation. Consequently, no contamination occurs from including validation or test samples in the synthesis process.

As shown in Table 3, the ViT-based models exhibit limited performance, which is expected given that vision transformers require substantially larger datasets to learn stable representations. The limited size and severe class imbalance negatively affect their ability to generalize. In contrast, EfficientNet performs comparatively better. For all models, performance is higher in binary (malignant/benign) classification, reflecting the greater difficulty posed by the imbalance in multi-class settings.

Notably, incorporating MAE pretraining on synthetic data consistently improves the performance of ViT architectures. In particular, F1-based metrics benefit the most, as the inclusion of synthetic samples helps balance the dataset, enabling models to learn malignant features more effectively and distinguish between lesion types. Furthermore,

Table 1. Evaluation on HAM10000 for categorical and binary lesion classification. Results are shown for ViT-L and ViT-B baselines and their variants with MAE pretraining (MAE), synthetic data (synth), and knowledge distillation (distill). Comparisons include Derm-t2im [5] and EfficientNet baselines, as well as EfficientNet models augmented with MAE pretraining and distillation.

Model	Categorical		Malignant/Benign	
	ACC	F1	ACC	F1
ViT-L (Baseline)	0.6579	0.6383	0.7612	0.4043
ViT-B (Baseline)	0.6748	0.6498	0.7225	0.3209
EfficientNet-B0 [11]	0.7976	0.6726	0.8050	0.7563
EfficientNet-B3 [11]	0.7160	0.7184	0.8157	0.7330
EfficientNet-B7 [11]	0.7913	0.7470	0.8152	0.7361
Derm-t2im [5] (ViT)	-	-	0.8502	-
Derm-t2im [5] (MobileNet)	-	-	0.7358	-
ViT-B + synth	0.6719	0.6557	0.7952	0.7506
MAE + ViT-H + synth	0.8915	0.8911	0.8715	0.8715
MAE + ViT-L + synth	0.8382	0.8247	0.8512	0.8361
MAE ViT-H distill to ViT-B (no synth)	0.7719	0.7557	0.8782	0.8797
MAE ViT-H distill to ViT-B + (non-cond.) synth	0.7337	0.7216	0.8278	0.7887
MAE ViT-H distill to ViT-B + synth	0.8186	0.7225	0.8278	0.7887
MAE ViT-H distill EfficientNet-B0 + synth	0.8058	0.7563	0.9051	0.9010

when applying knowledge distillation (distill) from the MAE-pretrained teacher, and fine-tuning with a combination of real and class-conditioned synthetic samples (synth) generated by our diffusion model, both ViT-B and EfficientNet-B0 achieve additional gains. These results demonstrate the effectiveness of synthetic-data-driven pretraining and distillation in mitigating data scarcity and imbalance in dermatological image classification.

Figure 2 provides a qualitative comparison of the different synthetic image generation strategies. The results illustrate how the inclusion of perceptual loss enhances the visual fidelity and structural representation of skin lesions, while class conditioning further improves the realism and diversity of generated samples.

3.1. Performance considerations

The ViT-H provides strong representations but is impractical for mobile or edge deployment due to its high computational and memory demands ($\approx 2.5GB$ model size and $\approx 55 - 60GFLOPs$ per inference at 256×256 resolution). Although ViT-B reduces the parameter count by approximately $8 \times$ ($\approx 86M$ parameters), it remains costly for mobile devices, requiring approximately $17 - 18GFLOPs$ per inference. In contrast, knowledge distillation enables transferring the representational power of large transformers to lightweight architectures such as EfficientNet-B0, allowing efficient on-device inference with only $\approx 0.6GFLOPs$ and approximately $5M$ parameters.

4. CONCLUSION

We addressed class imbalance in skin lesion classification by integrating class-conditioned diffusion-based synthesis with

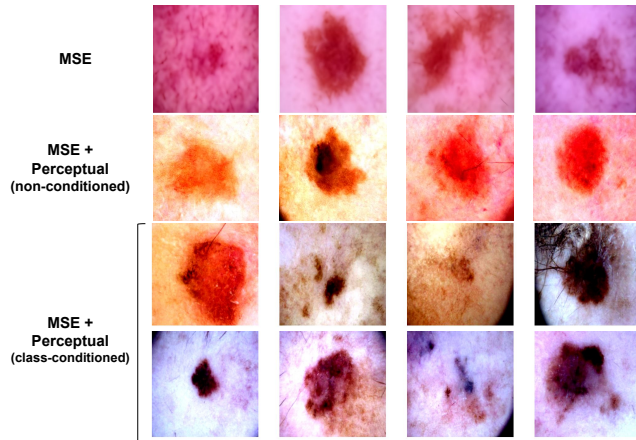


Fig. 2. Qualitative comparison of latent diffusion generation strategies. Rows (top to bottom): MSE loss, MSE + perceptual loss (unconditional), and MSE + perceptual loss (class-conditioned benign/malignant).

MAE pretraining and knowledge distillation. This strategy enables robust representation learning from limited dermatology datasets while allowing lightweight student models to retain strong discriminative performance for both benign and malignant lesions. Our results demonstrate the effectiveness of synthetic data and teacher-student training for efficient and deployable dermatology classification systems.

5. COMPLIANCE WITH ETHICAL STANDARDS

This research study was conducted retrospectively using human subject data made available in open access [8]. Ethical approval was not required, as confirmed by the attached license for the open-access data.

6. ACKNOWLEDGMENTS

This work was partially supported by INES.IA (National Institute of Science and Technology for Software Engineering Based on and for Artificial Intelligence) www.ines.org.br, CNPq grant 408817/2024-0. The project was supported by the Ministry of Science, Technology, and Innovation of Brazil, with resources from Law No. 8,248, dated October 23, 1991, under the scope of the PPI-SOFTEX, coordinated by Softex and published under RESIDÊNCIA EM TIC 63 – ROBÓTICA E IA – FASE II, DOU 23076.043130/2025-27.

7. REFERENCES

[1] Matthew W Tsang and Jack S Resneck Jr, “Even patients with changing moles face long dermatology appointment wait-times: a study of simulated patient calls

to dermatologists,” *Journal of the American Academy of Dermatology*, vol. 55, no. 1, pp. 54–58, 2006.

- [2] Hongwei Ding, Nana Huang, Yaoxin Wu, and Xiaohui Cui, “Improving imbalanced medical image classification through gan-based data augmentation methods,” *Pattern Recognition*, vol. 166, pp. 111680, 2025.
- [3] Aniket Patil, Anjula Mehto, and Saif Nalband, “Enhancing skin lesion diagnosis with data augmentation techniques: a review of the state-of-the-art,” *Multimedia Tools and Applications*, vol. 84, no. 22, pp. 25325–25364, 2025.
- [4] Fábio Perez, Cristina Vasconcelos, Sandra Avila, and Eduardo Valle, “Data augmentation for skin lesion analysis,” in *International Workshop on Computer-Assisted and Robotic Endoscopy*. Springer, 2018, pp. 303–311.
- [5] Muhammad Ali Farooq, Wang Yao, Michael Schukat, Mark A Little, and Peter Corcoran, “Derm-t2im: Harnessing synthetic skin lesion data via stable diffusion models for enhanced skin disease classification using vit and cnn,” in *2024 46th Annual International Conference of the IEEE Engineering in Medicine and Biology Society (EMBC)*. IEEE, 2024, pp. 1–5.
- [6] Jonathan Ho, Ajay Jain, and Pieter Abbeel, “Denoising diffusion probabilistic models,” *Advances in neural information processing systems*, vol. 33, pp. 6840–6851, 2020.
- [7] Hugo Touvron, Matthieu Cord, Matthijs Douze, Francisco Massa, Alexandre Sablayrolles, and Hervé Jégou, “Training data-efficient image transformers & distillation through attention,” in *International conference on machine learning*. PMLR, 2021, pp. 10347–10357.
- [8] Philipp Tschandl, Cliff Rosendahl, and Harald Kittler, “The ham10000 dataset, a large collection of multi-source dermatoscopic images of common pigmented skin lesions,” *Scientific data*, vol. 5, no. 1, pp. 1–9, 2018.
- [9] Justin Johnson, Alexandre Alahi, and Li Fei-Fei, “Perceptual losses for real-time style transfer and super-resolution,” in *European Conference on Computer Vision (ECCV)*, 2016.
- [10] Kaiming He, Xinlei Chen, Saining Xie, Yanghao Li, Piotr Dollár, and Ross Girshick, “Masked autoencoders are scalable vision learners,” in *2022 IEEE/CVF Conference on Computer Vision and Pattern Recognition (CVPR)*, 2022, pp. 15979–15988.
- [11] Mingxing Tan and Quoc Le, “Efficientnet: Rethinking model scaling for convolutional neural networks,” in *International conference on machine learning*. PMLR, 2019, pp. 6105–6114.